Exploring Protein Conformational Landscapes Using High-Pressure NMR

Julien Roche[*], Catherine A. Royer[†,1], Christian Roumestand[‡]

*Roy J. Carver Department of Biochemistry, Biophysics and Molecular Biology, Iowa State University, Ames, IA, United States
†Department of Biological Sciences, Rensselaer Polytechnic Institute, Troy, NY, United States
‡Centre de Biochimie Structural CNRS Université de Montpellier UMR, Montpellier, France
1Corresponding author: e-mail address: royerc@rpi.edu

Contents

Abstract

Protein conformational landscapes define their functional properties as well as their proteostasis. Hence, detailed mapping of these landscapes is necessary to understand and modulate protein conformation. The combination of high pressure and NMR provides a particularly powerful approach to characterizing protein conformational transitions. First, pressure, because its effects on protein structure arise from elimination of solvent excluded void volume, represents a more subtle perturbation than chemical denaturants, favoring the population of intermediates. Second, the residue-specific and multifaceted nature of NMR observables informs on many local structural properties of proteins, aiding in the characterization of intermediate and excited states.
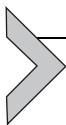
1. INTRODUCTION

The sequences of extant biological macromolecules (proteins and nucleic acids) have evolved to allow their functional properties to confer a requisite competitive advantage on the organisms in which they are found, for the environmental conditions in which these organisms live. While homologues of the same proteins across all organisms in which they are produced adopt the same or quite similar structures, their global stabilities, and perhaps even more importantly, the degree to which they populate intermediate or excited state structures can vary considerably. These excited states or intermediate structures can play central roles in biomolecular function. For example, in the case of proteins, local unfolding or complex dissociation may be required for or coupled to interaction with ligand or substrate. Posttranslational modification probability likewise may differ significantly for different conformational states of proteins. Such modifications can impact protein localization or turnover, and hence modulate their functional and/or proteostasis properties. It is increasingly recognized that selective pressure on entire conformational landscapes has modulated protein and nucleic acid sequences. However, while the understanding of how sequence impacts global biomolecular stability has progressed a great deal in recent years, much less is known about how sequence modulates these conformational landscapes. In this chapter, we discuss high-pressure NMR as a particularly useful methodology for exploring biomolecular conformational landscapes, and the effects of changes in sequence thereon. We will focus on protein folding landscapes, with some discussion of protein association. However, this methodology can be applied to nucleic acid conformational landscapes as well.

Much of the information obtained to date concerning protein folding mechanisms comes from folding/unfolding experiments performed in vitro. Several perturbation methods can be used to modulate protein stability: adding chemical denaturants (urea, guanidinium chloride, GuHCl) or stabilizers (osmolytes such as sucrose or glycerol), changing the pH, or modifying the thermodynamic parameters of the sample (pressure, temperature). While most protein folding studies have used chemical denaturants, pH, or temperature, pressure presents a number of advantages and can provide complementary information to that obtained using the more common perturbation approaches. The temperature dependence of protein stability is complex, with a strong temperature dependence of both the enthalpy and entropy change upon folding due to the large difference in heat

capacity between the folded and unfolded states (Privalov & Gill, 1988). Chemical denaturation (or stabilization) is directly related to the preferential interaction (or exclusion) of the additive, and thus depends upon the absolute difference in exposed surface area between the folded and unfolded states. This in turn is simply correlated with the size of the protein (Myers, Pace, & Scholtz, 1995), as is the change in heat capacity. Changing pH can have interesting effects, as the change in stability depends on the local pK_a values of ionizable residues. Pressure, while relatively little employed, is actually a very straightforward perturbation. Pressure-induced unfolding occurs because the molar volume of the folded states of proteins is larger than that of their unfolded states. We demonstrated recently (Roche, Caro, et al., 2012; Rouget et al., 2011) that this effect was primarily due to the existence within folded protein structures, of solvent excluded void volume that is eliminated in the unfolded form. The difference in volume, ΔV_f, is present at atmospheric pressure. All that pressure does, per Le Chatelier's principle, is to shift the $F \leftrightarrow U$ equilibrium toward the lower volume, unfolded state. Given this mechanism for pressure effects on protein stability, its effects, like pH, can be "local." That is, for comparable stabilities, protein regions or domains that are less well packed will be more pressure sensitive than more tightly packed regions. Another consequence of these volumetric effects is that single amino acid substitutions can drastically alter susceptibility to pressure (Ando et al., 2008; Roche, Caro, et al., 2012). In contrast to pH, denaturants, and high temperature, which are highly disruptive, pressure will only act to eliminate internal void volume, such that pressure unfolded states may be less disrupted than those observed using these other methods of denaturation (Rouget et al., 2011; Zhang et al., 2018).

Thus, in spite of some difficulties in implementation, most of which have been adequately addressed in available commercial instrumentation, pressure represents a method of choice to study protein folding. Generally, unfolding by pressure is reversible, most prominently because high pressure disfavors intermolecular protein interactions, such that irreversible aggregation is most often avoided. Moreover, pressure is a continuous variable, requiring a single sample for the entire unfolding (and refolding) profile. This reversibility gives access to a large panel of thermodynamic parameters specific to the folding/unfolding reaction (Akasaka, Kitahara, & Kamatari, 2013; Kamatari, Kitahara, Yamada, Yokoyama, & Akasaka, 2004). Pressure perturbation is generally used in conjunction with spectroscopic methods, such as circular dichroism, fluorescence, or IR spectroscopy (Dellarole & Royer, 2014). These observables yield global information on the evolution of the tertiary or secondary structure during protein unfolding. Due to its

extreme sensitivity to structural perturbations, nuclear magnetic resonance (NMR) constitutes an attractive alternative observable, particularly in conjunction with a continuous variable such as pressure. Although 1D NMR can provide global information on protein folding thermodynamics, the multiple probes available through multidimensional NMR give access to local, residue-specific information. Thus, the combination of high pressure and NMR constitutes a powerful tool that can lead to new knowledge concerning the role of residue packing in protein stability, of conformational fluctuations in water penetration, or that can be used to describe folding intermediates or other details of the conformational landscape, which cannot be accessed by global spectroscopic observables.

2. MONITORING "GLOBAL" FOLDING/UNFOLDING REACTIONS WITH 1D HIGH-PRESSURE NMR SPECTROSCOPY

The NMR resonances (or chemical shifts) of magnetically active nuclei (^{1}H, ^{15}N, ^{13}C) in a protein are extremely sensitive to the through-space effects of neighboring groups: this leads to the good dispersion usually observed in the NMR spectrum of a folded protein. When the protein unfolds, these through-space effects are largely eliminated: the NMR resonances become almost uniquely sensitive to through-bond effects between covalently bound atoms. As a consequence, the NMR spectrum collapses and becomes poorly resolved (Fig. 1). For instance, since they are borne by the same chemical groups, all the ^{1}H resonances of the methyl groups, or of the amide groups of the amino acids in a protein will give rise to almost identical resonances, with only slight variations due to differences in the chemical nature of the 20 amino acid side chains. Thus, it is possible to monitor the high-pressure denaturation of a protein by following the evolution of its 1D NMR spectrum, as depicted in Fig. 1 for Titin I27 domain, a protein for which folding has been extensively studied. As generally observed, folded and unfolded species are in slow exchange with regard to the NMR timescale: we do not observe chemical shift variations, indicative of fast exchange, as a function of pressure, but rather the disappearance of resonances belonging to the native form, with the concomitant appearance of new peaks that correspond to the spectrum of the unfolded species with a similar chemical environment for all residues. Note than coupling high-pressure and NMR raises complicated technological issues. The
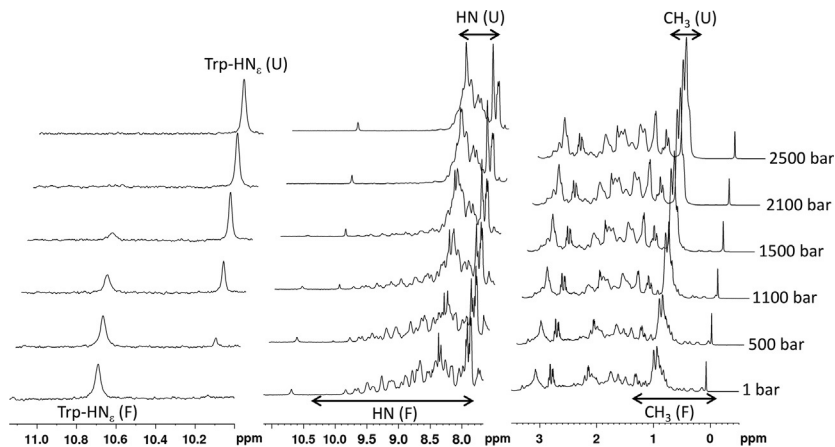
Fig. 1 Monitoring the pressure unfolding of Titin I27 domain with 1D NMR spectroscopy. Stacked plot of 1D spectra (amide and aliphatic regions) recorded at 600 MHz on a sample of Titin I27 domain (1 mM in Tris buffer pH 7.0, 298 K, 1.7 M GuHCl) as a function of pressure. The regions corresponding to HN amide and CH_3 methyl group resonances in the folded (F) and unfolded (U) states are indicated with *arrows*. The decrease of the resonances corresponding to the HN of Trp-34 in the folded state with the concomitant increase of the same resonances in the unfolded state is also shown (*left*).

experimental device should of course support high pressure but must be nonmagnetic and permeable to radiofrequency. A satisfying commercial solution has emerged, based on the use of ceramic tubes (zirconium oxide) developed by the Wand group (Peterson & Wand, 2005) and now available commercially (Daedalus Innovations™). These tubes can support up to 300 MPa (3 kbar), usually enough to unfold protein. If proteins are too stable to be unfolded by pressure over this range, one can adjust the protein stability, generally by shifting the temperature or adding low concentration of chaotropic reagents. For instance, in the case of Titin I27 domain (Fig. 1), 1.7 M of GuHCl has been added to the protein solution in order to allow complete unfolding in the range 1–2500 bar. The ceramic high-pressure NMR tubes can be used in combination with any commercial NMR probe and maintain a sensitivity of ~50% relative to that obtained with classical 3 mm Borosilicate or Pyrex glass tubes.

Often, the decrease of the composite peaks corresponding to the folded (F) conformation, or the increase of peaks corresponding to the unfolded states (U), with pressure follows a sigmoidal curve characteristic of a two-state equilibrium (Fig. 2), in the form of:
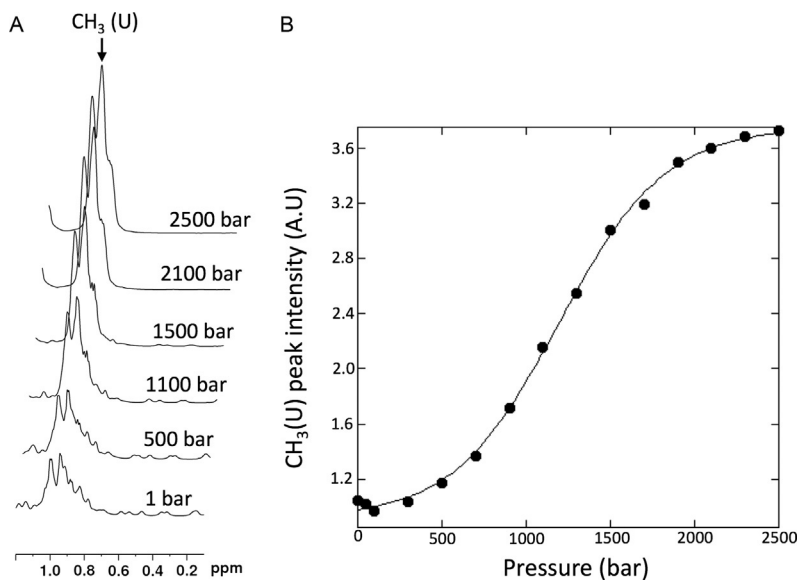
Fig. 2 Measuring steady-state thermodynamic parameters form 1D NMR spectroscopy. (A) Stacked plot of the methyl resonance region of 1D spectra recorded on a sample of Titin I27 domain as a function of pressure (same conditions as stated in Fig. 1). The *arrow* indicates the line corresponding to the methyl resonances in the unfolded species (*U*). (B) Fit of the sigmoidal increase of the methyl resonances of the unfolded state with pressure using Eq. (6).

$$F \underset{k_f}{\overset{k_u}{\rightleftarrows}} U$$

with a characteristic equilibrium constant of:

$$K_{eq} = \frac{k_f}{k_u} = \frac{[U]}{[F]} \tag{1}$$

where k_f and k_u stand for the folding and the unfolding rate constants. K_{eq} can be also expressed from the Boltzmann equation as:

$$K_{eq} = \exp\left(\frac{-\Delta G_{eq}}{RT}\right) \tag{2}$$

where the free energy change can be expressed as a Taylor expansion, truncated at the second order term:

$$\Delta G_{eq} = G_U - G_F = \Delta G^0 + \Delta V^0(p - p_0) - \frac{1}{2}\Delta\beta V^0(p - p_0)^2 + \dots \tag{3}$$

Here ΔG and ΔG^0 are the Gibbs free energy changes from F to U at pressure p and p_0 ($p_0 = 0.1\,\mathrm{MPa}$), respectively; ΔV^0 is the partial molar volume change; $\Delta\beta \,(= -(1/V^0) * \delta V/\delta p)$ is the change in compressibility coefficient, R is the gas constant, and T is the absolute temperature. For proteins the differences in compressibility between native and denatured states are negligible (Ravindra & Winter, 2003). Hence, the expression of ΔG simplifies to:

$$\Delta G_{eq} = \Delta G^0 + \Delta V^0 (p - p_0) \tag{4}$$

The observable will be I, the intensity (or integral) of a peak corresponding to either the folded species or of the unfolded species. In the case of Titin I27 domain, we chose to follow the increase of a peak corresponding to methyl groups corresponding to the unfolded species (Fig. 2). Thus, the equilibrium constant can be written as:

$$K_{eq} = \frac{[U]}{[F]} = \frac{I_F - I}{I - I_U} \tag{5}$$

where, for a given residue, I_F stands for the intensity of the corresponding NMR line in the folded spectrum at 1 bar ($I_F = I_{min}$), while I_U corresponds to the intensity of the same line at high pressure, when the protein is fully unfolded ($I_U = I_{max}$) for the unfolded state methyl peaks. Combining this equation with Eqs. (2) and (4) gives the characteristic equation for a two-state equilibrium:

$$I = \frac{I_F + I_U e^{-[\Delta G^0 + (p-p_0)\Delta V^0]/RT}}{1 + e^{-[\Delta G^0 + (p-p_0)\Delta V^0]/RT}} \tag{6}$$

Fitting the data plotted in Fig. 2 for Titin I27, we can extract "global" values for ΔV^0 of unfolding ($-75\,\mathrm{mL/mol}$) and ΔG^0 (2.5 kcal), under the conditions of the study (pH 7, 25°C, 1.7 M GuHCl). Generally, uncertainties on the recovered parameters depend upon, not only the quality of the data, but also on how well-defined are the low- and high-pressure plateau regions. Typically, uncertainty on the free energy and volume changes of unfolding are between 5% and 10%.

The parameters ΔV^0 and ΔG^0 are characteristics of the system at equilibrium, at atmospheric pressure. A complete understanding of the protein folding/unfolding phenomenon requires a temporal description of the reaction to obtain information concerning the folding barrier. Such a description relies on the measurement of kinetic parameters, after perturbation of the

thermodynamic equilibrium between the folded and unfolded conformers of the protein. In addition, these studies yield the rates of folding and unfolding under native conditions and the activation volume measured between the unfolded state or the folded state and the transition state ensemble (TSE), $\Delta V_f^{\ddagger}$ and $\Delta V_u^{\ddagger}$, respectively.

When applied to the complete unfolding/folding transition, high-pressure can slow down the rate of folding (Vidugiris, Markley, & Royer, 1995), and also possibly unfolding (Rouget et al., 2011), by several orders of magnitude due to the very large volumes of activation involved in these reactions. Thus, a reaction completed in few seconds at atmospheric pressure can take several minutes to even a few hours to relax at higher pressure. For example, $\Delta + PHS$ SNase at pressure above 1 kbar exhibits residue-specific relaxation times greater than 10 h (Roche, Caro, et al., 2012). It becomes thus feasible to monitor the unfolding kinetics using 1D real-time NMR. In the case of Titin I27, we used pseudo-2D experiments to measure the relaxation times after different p-jump (Fig. 3A and B). They consist in a series of 1D NMR spectrum recorded at a constant repeating rate. After Fourier transform along the acquisition dimension, one can extract from the matrix obtained a column at a chemical shift corresponding, for instance, to the methyl groups of the unfolded states. In that case, we observe an exponential rise of this resonance with time, from which the relaxation time ($\tau = 1/(k_u + k_f)$) can be extracted. It is possible to extract the values of k_u and k_f, as well as those of the activation volume of unfolding $\Delta V_u^{\ddagger}$ (or folding, $\Delta V_f^{\ddagger}$) by measuring this relaxation time $\tau_{(p)}$, after different p-jumps in the pressure range where unfolding appears. The p-jump amplitude should be sufficient to observe a measurable intensity change for the NMR resonance but should remain moderate to avoid any imbalance between the folding and the unfolding reactions: an excessive positive p-jump, for instance, will favor the unfolding reaction at the expense of the folding reaction. For Titin I27, we have used pressure jumps of 200 bar, which is about 10% of the pressure range needed to fully unfold the protein (2000 bar).

With $\tau_{(p)} = 1/(k_u + k_f)$ and $k_f(p) = k_{f0}e^{-p\Delta V_f^{\ddagger}/RT}$ and $k_u(p) = k_{u0}e^{-p\Delta V_u^{\ddagger}/RT}$, $\tau_{(p)}$ can be rewritten as:

$$\tau_{(p)} = \left[k_{u0}e^{\left(\frac{-p\Delta V_{u0}^{\mp}}{RT}\right)} + k_{f0}e^{\left(\frac{-p\Delta V_{f0}^{\mp}}{RT}\right)} \right]^{-1} \tag{7}$$

Knowing the value of ΔV_{eq}, the volume difference between the folded and unfolded states measured at equilibrium ($\Delta V_{eq} = \Delta V_f - \Delta V_u$), and
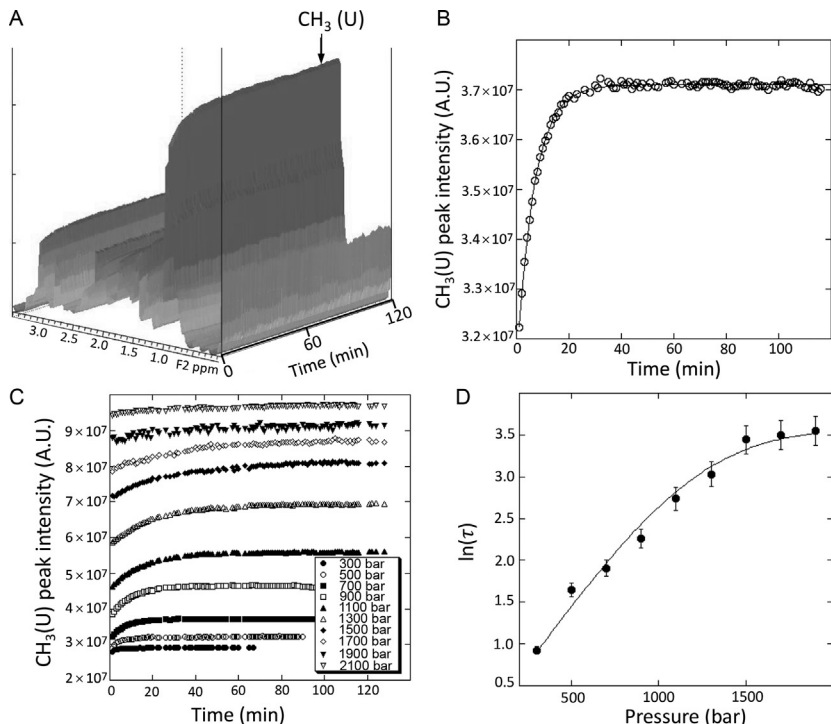
Fig. 3 Measuring the unfolding relaxation time after a *p*-Jump 1D NMR spectroscopy. (A) Series of 1D spectra of Titin I27 domain (same conditions as stated in Fig. 1) recorded with time after a 200 bar *p*-Jump (500 → 700 bar). Sixty spectra of 2 min each were recorded over a period of 2 h. The position of the resonance corresponding to methyl groups in the unfolded species is indicated with an *arrow*. (B) Fit of the exponential rise of this methyl resonance, allowing the measurement of the relaxation time, τ, at 700 bar. (C) Exponential rises of the resonance corresponding to the methyl groups in the unfolded states after successive 200 bar *p*-Jumps between 300 and 2100 bar, the pressure range where Titin I27 unfolds. Relaxation times $\tau_{(p)}$ can be measured from these experiments for the different pressures. (D) "Chevron plot" of the natural logarithm of τ at different pressures: the fit with Eq. (8) allows to extract the kinetic constants k_u and k_f, as well as the activation volume of folding $\Delta V_{f0}^{\ddagger}$ or of unfolding $\Delta V_{u0}^{\ddagger}$ at atmospheric pressure.

$K_{eq} = k_f/k_u$, one can constrain the fit and decrease the number of parameters. Eq. (7) becomes:

$$\tau_{(p)} = \left[k_{u0} e^{\left(\frac{-p \Delta V_{u0}^{\mp}}{RT} \right)} + k_{u0} K_{eq} e^{\left(\frac{-p \left(\Delta V_{eq} + \Delta V_{u0}^{\mp} \right)}{RT} \right)} \right]^{-1} \qquad (8)$$

Only two variables need to be fitted: k_{u0} (the unfolding rate at atmospheric pressure) (or folding, k_{f0}) and $\Delta V_{u0}^{\ddagger}$ (the activation volume for unfolding at atmospheric pressure) or ΔV_{0f} (Fig. 3C). Generally, it is advantageous to fit for the parameters (folding or unfolding) which are most affected by pressure. The fit is usually performed on a plot of $\ln(\tau)$ as a function of pressure that presents the characteristic pattern of a "chevron plot" (Fig. 3D). In the case of Titin I27, we measured an activation volume $\Delta V_f^{\ddagger}$ close to the equilibrium ΔV^0 value, indicating that the molar volume of the transition state is quite close to that of the folded state, suggesting a dehydrated TSE where most of the native cavities are still present. The intrinsic limitation of this approach resides in the fact that while NMR has high spatial resolution, its time resolution is limited: the recording time of a 1D NMR spectrum ranges from few seconds to 1–2 min, depending on the sample concentration. Thus, such experiments can be used only in the case of proteins having slow relaxation times, above 5–10 min. In the case of protein having fast relaxation times (<1 s), other NMR approaches are available, mainly based on 2D exchange spectroscopy techniques. They will be discussed in details in a later section.
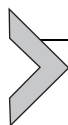
3. MONITORING "LOCAL" PROTEIN FOLDING/ UNFOLDING REACTION WITH HIGH-PRESSURE 2D NMR SPECTROSCOPY: EXPLORING THE FOLDING LANDSCAPE

In many of the studies reported in the literature, and whatever the spectroscopy used (Fluorescence, IR, CD, or NMR), the folding/unfolding reaction of a protein can be approximate by a two-state model, excluding the possibility of any folding intermediates in the folding energy landscape of a protein. This is of course a rough approximation: most globular proteins are known to deviate from a true two-state folding mechanism and an ideal global cooperativity by populating en route folding intermediate states, underlying the concept of "foldons" (Englander, Mayne, & Krishna, 2007; Lindberg & Oliveberg, 2007). This apparent discrepancy is essentially due to the low stability of the intermediate states which are often only transiently populated, with no detectable equilibrium population. Moreover, often the spectroscopic observable gives access only to global "apparent" values for thermodynamic parameters (ΔG^0 and ΔV^0 or m-value). Deviations from two-state behavior manifest as smaller values for the thermodynamic parameters, yet without prior knowledge of the true global stability and cooperativity, such deviations from two-state behavior

are often not recognized. For example, in the case of Titin I27, ΔG^0 and ΔV^0 values measured from the pressure dependence of the resonance corresponding to the unfolded state methyl groups or to the indole NH of the tryptophan side chain in the denatured state are significantly different (72 ± 8 vs 83 ± 5 mL/mol), indicating deviation from true two-state behavior. Multiple probes allow a more complete description of the folding/unfolding process.

Multidimensional NMR spectroscopy is able to provide residue-specific information, through correlation spectroscopy involving nuclei located on the peptide backbone (^{1}H and ^{15}N of amide groups, Hα and Cα), allowing a residue-specific analysis of the folding process. Thus, the atomic resolution offered by NMR experiments provides an intrinsic multiprobe approach to assess the degree of protein folding cooperativity, which is otherwise difficult to characterize using techniques such as circular dichroism or fluorescence. Amide protons offer ideal probes to monitor the unfolding reaction: each amino acid (with the exception of proline) bears an NH group, and the corresponding proton resonances represent the most resolved region of the proton spectrum of a protein. This resolution can be considerably enhanced through homonuclear (COSY, TOCSY, NOESY) or heteronuclear ([^{1}H–^{15}N]-HSQC) experiments. In addition, their acidic character makes these amide protons well suited for proton/deuteron exchange measurements, a property that has been extensively used to evaluate the local stability of a protein, with a possible association with high pressure, as will be discussed further. Series of [^{1}H–^{15}N] HSQC can also be used to monitor the dissociation of protein complexes induced by pressure. This was applied for the HIV-1 protease for which the monomer–dimer exchange occurs on a slow time scale (Ishima, Torchia, & Louis, 2007). At low enough concentration, both the dimer and monomer cross-peaks can be simultaneously monitored as a function of pressure and the intensity profiles of interfacial residues can be fitted to calculate the relative population of dimer, monomer, and unfolded states at each pressure (Louis & Roche, 2016). These experiments allow the determination of the binding affinity of the dimer at atmospheric pressure and the volume change associated with the pressure-induced dissociation of the dimer (Louis & Roche, 2016).

3.1 Tracking Intermediate States in the Protein Folding Landscape

The pressure-induced unfolding reaction, which occurs on a slow timescale with respect to NMR, is often analyzed by monitoring the decrease in volume or intensity of native state cross-peaks in a series of [^{1}H–^{15}N]-HSQC
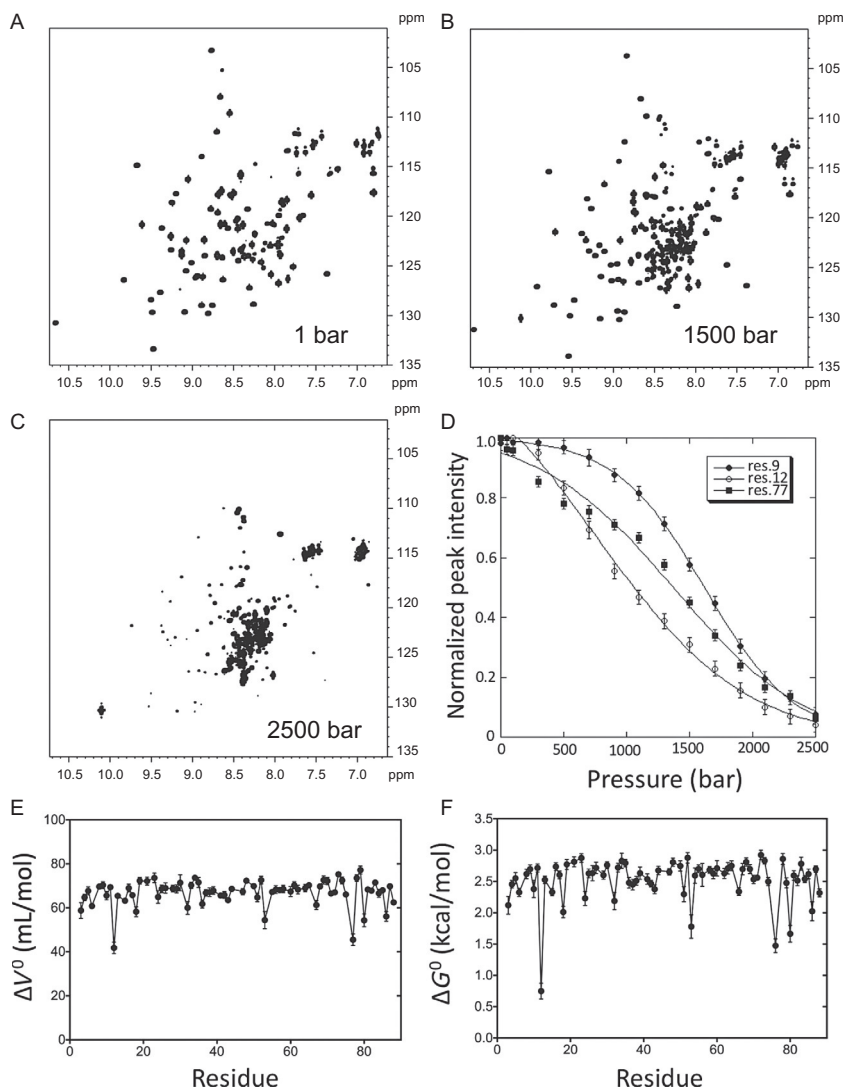
Fig. 4 2D NMR detected high pressure unfolding of Titin I27 domain. (A–C) Examples of [^{1}H–^{15}N] HSQC NMR spectra recorded on a ^{15}N-labeled sample of Titin I27 at different pressures as indicated. (D) Examples of three residues exhibiting distinct unfolding profiles. (E) Residue-specific ΔV^0 and (F) ΔG^0 measured at equilibrium from pressure unfolding of Titin I27 domain.

experiments recorded at increasing pressure (Fig. 4A–C). Of course, to extract the most useful information from these HP 2D NMR experiments, the cross-peaks must be assigned to specific residues in the protein sequence. Care must be taken that these measurements be recorded when the

equilibrium between native/unfolded populations has been reached after a pressure-jump: the pseudo-2D experiments described earlier can be readily used to evaluate the value of the relaxation time τ needed to reach equilibrium. Moreover, since the intensity (or integral) of each amide NH cross-peak is taken to represent the population of a conformational ensemble in which that amide resonance is in the chemical environment of the folded state, it is important to minimize loss of intensity due to experimental artifacts. In particular, it is important to choose a delay time between scans that is ~fivefold longer than the longitudinal relaxation time, T_1. Thus, T_1 should be measured (e.g., by inversion recovery) at atmospheric pressure for each sample at the temperature and under the solution conditions of the HP experiment to be performed. While T_1 can vary strongly with temperature, we have found that for proteins and nucleic acids proton T_1 values are pressure independent. Thus, the T_1 measurement need not be made as a function of pressure.

The residue-specific pressure-dependent peak volume or intensity values can be analyzed by individually fitting using Eq. (6), yielding residue-specific apparent ΔV_u^0 and ΔG_u^0 values (Roche, Caro, et al., 2012; Roche, Dellarole, Royer, & Roumestand, 2015; Roche, Louis, Bax, & Best, 2015) (Fig. 4D). Unlike the composite 1D methyl proton resonances of the unfolded state or fluorescence or CD, these 2D (usually $^{15}N–^1H$ HSQC) residue-specific profiles generally correspond to apparent two-state transitions, at least locally. This is because the resonance is either at the frequency observed for the folded state or it is not, in which case the intensity of the "folded state" peak decreases. Note that these "folded state" peaks shift somewhat with pressure due to compression and small conformational changes in the "folded state" ensemble. These shifts have been investigated for many proteins (for example, see Akasaka, 2006), and it has been shown recently that to a large extent these shifts are due to solvent-induced polarization of the backbone (Frach et al., 2016).

In contrast, here we are concerned with the disappearance of the "folded state" peaks as the protein populates conformational states in which the chemical environment of the residues is more strongly modified, leading to a loss of "folded state" peak intensity. Note that the high-pressure plateau of the folded state (whether it is attained or not in the experiment) should be equal to zero since at some pressure all conformers in which a residue is in its "folded state" environment should be eliminated. Thus, even if that high-pressure plateau is not attained due to experimental limitations of the apparatus, for example, in many cases fixing the high-pressure plateau value (I_U in Eq. 6) to a value of zero in the fits allows for a reasonable estimation of

the apparent thermodynamic parameters. Note that usually one fits the decrease of the cross–peaks for residues in the "folded state," instead of the sigmoidal increase of cross–peaks in the "unfolded state." This is because (i) the NMR spectra of the folded protein are usually assigned, which is rarely the case for the unfolded species and (ii) the NMR spectra of folded protein show usually a better dispersion, facilitating the analysis. In some cases, the unfolded state peaks can be accessed. We have done so for the unfolded state indole NH peak of for tryptophan in single tryptophan containing proteins (Zhang et al., 2018), and as noted above in the 1D spectrum of Titin I27. This information is quite useful as this peak is generally in slow exchange with that corresponding to the folded state. Moreover, both of these profiles (Trp indole "F" and "U") can be compared to that obtained using fluorescence from the same residue. Such comparisons can bring to light the population of intermediate species. In addition, the unfolded state peaks for glycine residues are often also easy to quantify. Even in the absence of assignments for these peaks, and depending on the protein's sequence, they can yield useful information when compared to the loss of "folded state" glycine peaks (Zhang et al., 2018).

Large variations in the ΔV^0 and ΔG^0 values measured for different residues of a given protein typically reflect departure from a two–state unfolding transition and inform on the potential presence of intermediate states as observed for $\Delta+$PHS staphylococcal nuclease (Snase), Titin I27, and a variant of the pp32 leucine-rich repeat protein in which the N-terminal capping motif has been deleted (pp32-ΔNcap) (Louis & Roche, 2016; Roche, Caro, et al., 2012; Zhang et al., 2018). In the case of Titin I27, for example, while most of the residues in the Titin I27 protein exhibit a similar ΔV^0 for unfolding of ≈ -70 mL/mol, in some areas of the protein the measured residue-specific ΔV^0 values fall below this average value (<55 mL/mol) (Fig. 4E), meaning that some regions of the protein unfold before others, suggesting the presence of folding intermediates, i.e., partially folded conformers having some degree of stability, in the protein energy landscape (Fig. 4F).

Structural and energetic information about the folding intermediates can also be extracted from the pressure-dependent multidimensional NMR data (de Oliveira & Silva, 2015; Roche, Caro, et al., 2012; Roche, Dellarole, et al., 2012) using the following procedure inspired by the analysis method used by Munoz and coworkers to characterize the thermal unfolding of the downhill protein BBL (Naganathan & Munoz, 2008; Sadqi, Fushman, & Muñoz, 2006). After normalizing the residue-specific denaturation curves

obtained from the amide cross-peak intensity decays measured on the HSQC experiments recorded at variable pressure (see Fig. 5D), the value of 1 for a given cross-peak ($I = I_F = 1$) can be associated with a probability of 1 (100%) for the corresponding residue to be in the native state, with all the native contacts present. Similarly, a residue for which, at the same pressure, the corresponding cross-peak has disappeared ($I = I_U = 0$) from the HSQC spectrum has a probability equal to 0 to be in a native state: it belongs to an unfolded state where all the native contacts are lost. Now, we consider two residues i and j in an intermediate situation where the probability to be in a folded state are $P(i)$ and $P(j)$, respectively, at a given pressure. If these two residues are in contact in the native state, we assume the probability $P(i,j)$ to be in contact at this pressure to be given by the geometric mean (Fossat et al., 2016) of the individual probabilities $P(i,j) = [P(i) \times P(j)]^{0.5}$. Pressure-dependent contact maps can be constructed based on the contact map of the folded protein. These folded state contact maps are constructed from the 3D crystal or NMR structure of the protein by measuring all contacts between different atoms: usually, only the distances between Cα atoms of the different residues are used. These contacts are then plotted in a diagonal diagram with the protein sequence numbering on the X and Y axis). It is now possible to use a color code (for example) in order to report
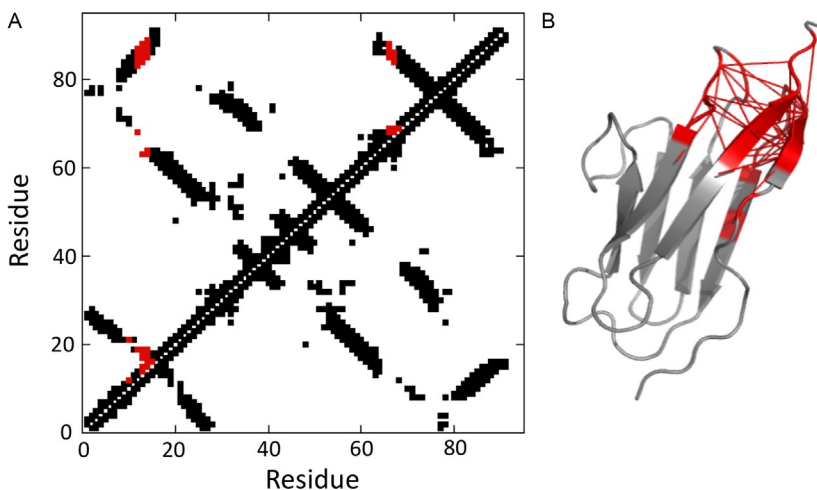

Fig. 5 Pressure denaturation of Titin I27 domain. (A) Contact maps built from the NMR structure of Titin I27 domain. The contacts above the diagonal have been colored in *red* when contact probabilities (P_{ij}) lower than 0.5 are observed at a pressure of 800 bar. (B) *Ribbon representations* of the structure of I27 where the *red ticks* represent contacts that are weakened ($P_{ij} \leq 0.5$) at 800 bar.

in this contact map the pressure–dependent probability of contact, as defined earlier (Fig. 5).

The strong deviation from two–state behavior in the HSQC-detected high–pressure unfolding of pp32 ΔN–cap (Zhang et al., 2018) provides another example of deducing some of the structural properties of folding intermediates using fractional contacts (Fig. 6). The N-terminal capping motif (yellow in Fig. 6A) provides stability to the WT protein (Dao, Majumdar, & Barrick, 2014), but CD-detected urea melts of the ΔN-cap variant showed no evidence for the strong deviation from two-state
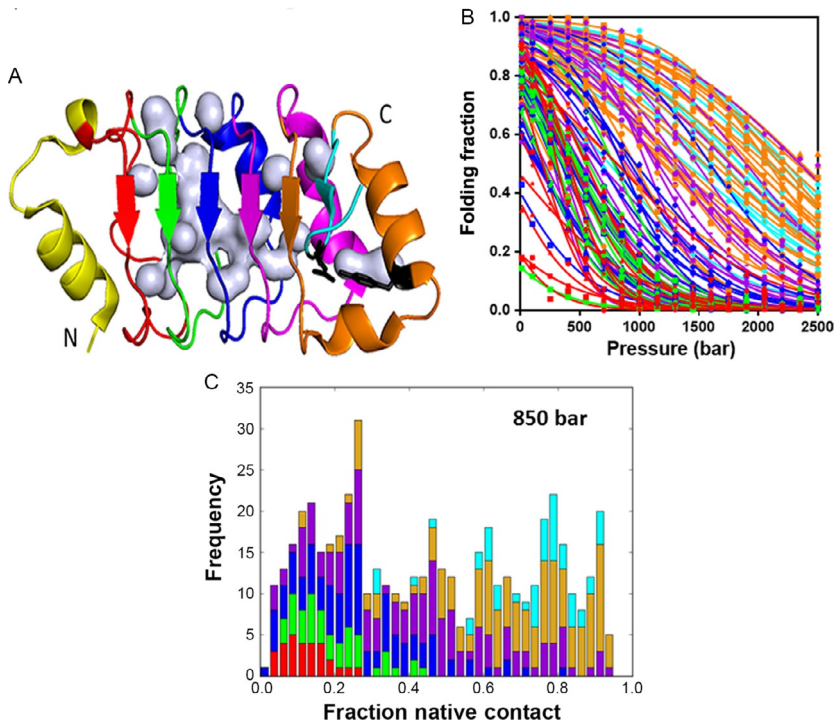

Fig. 6 HSQC-detected pressure denaturation of pp32 ΔN-cap. (A) Schematic of the protein in which the repeats and capping motifs are color coded. The N-cap (*yellow*) is deleted in the pp32 ΔN-cap variant. (B) Pressure-dependent loss of amide HSQC peak intensities for pp32 ΔN-cap. *Curves* are colored following the color scheme in (A). (C) Fractional contact histogram for pp32 ΔN-cap at 850 bar. *Bars* are color coded for the repeat according to the scheme in (A). Interfacial contacts are reported twice. *Results are taken from Zhang Y., Berghaus M., Klein S., Jenkins K., Zhang S., McCallum S.A., et al. (2018) High-pressure NMR and SAXS reveals how capping modulates folding cooperativity of the pp32 leucine-rich repeat protein. Journal of Molecular Biology 430, 1336–1349.*

behavior exhibited in the pressure–dependent HSQC profiles of the "folded state" amide NH peaks (Fig. 6B). The fractional contact values at 850 bar represented as histograms colored per repeat (Fig. 6C) reveal that the N- to C-terminal stability gradient already apparent in WT pp32 (Fossat et al., 2016) is reinforced by deletion of the N-cap, leading to the population of multiple intermediate species. While the intensity of the "folded state" peaks for residues in the first repeat (red) has disappeared by 1 kbar, residues in the C-terminal repeat and capping motif (brown and cyan) retain fractional "folded state" peak intensity even at 2500 bar. The composite "unfolded state" methyl peak intensity in the 1D proton spectrum did not begin to increase until above 1 kbar. Hence the intermediates populated present molten globule-like properties. This illustrates the distinction between true thermodynamic ensembles, and the locally "folded" and "unfolded" states detected by HP HSQC. The residue-specific transitions observed for "folded state" HSQC peaks represent the transition from a true thermodynamic ensemble in which that residue's amide resonates at its native state frequency, and one in which it does not. In the case of pp32 ΔN-cap, for residues in the N-terminal repeat 1, this is a transition from the true folded state to one in which repeat 1 is disordered, but the others are not. The transition observed for residues in the C-terminal capping motif is from an intermediate ensemble in which repeats 1–3 are disordered, while those in the C-terminus are not to the high-pressure unfolded state.

   Fractional contact maps determined from pressure unfolding experiments can also be combined with Go-model simulations to obtain a structural representation of the conformal ensemble populated at high pressure. Native contact lists can be obtained from a contact map and used for molecular modeling, with the possibility to "weight" the probabilities of forming a native contact calculated at a given pressure. A large number of contact lists will be then generated, instead of one. For example, a contact between two residues associated to a probability of 0.8 will be randomly added to 80 lists out of 100. For example, if the contact probability is only 0.4, the corresponding contact will be present in 40 lists over 100. One independent MD simulation is then run for each contact list and the conformations generated by all the simulations are collectively analyzed. In the case of the protein Δ + PHS SNase, such analysis allowed us to identify a population of conformers corresponding to a folding intermediate where the C-terminal α–helix is disrupted whereas the N-terminal β-barrel maintains its native structure (Fig. 7).
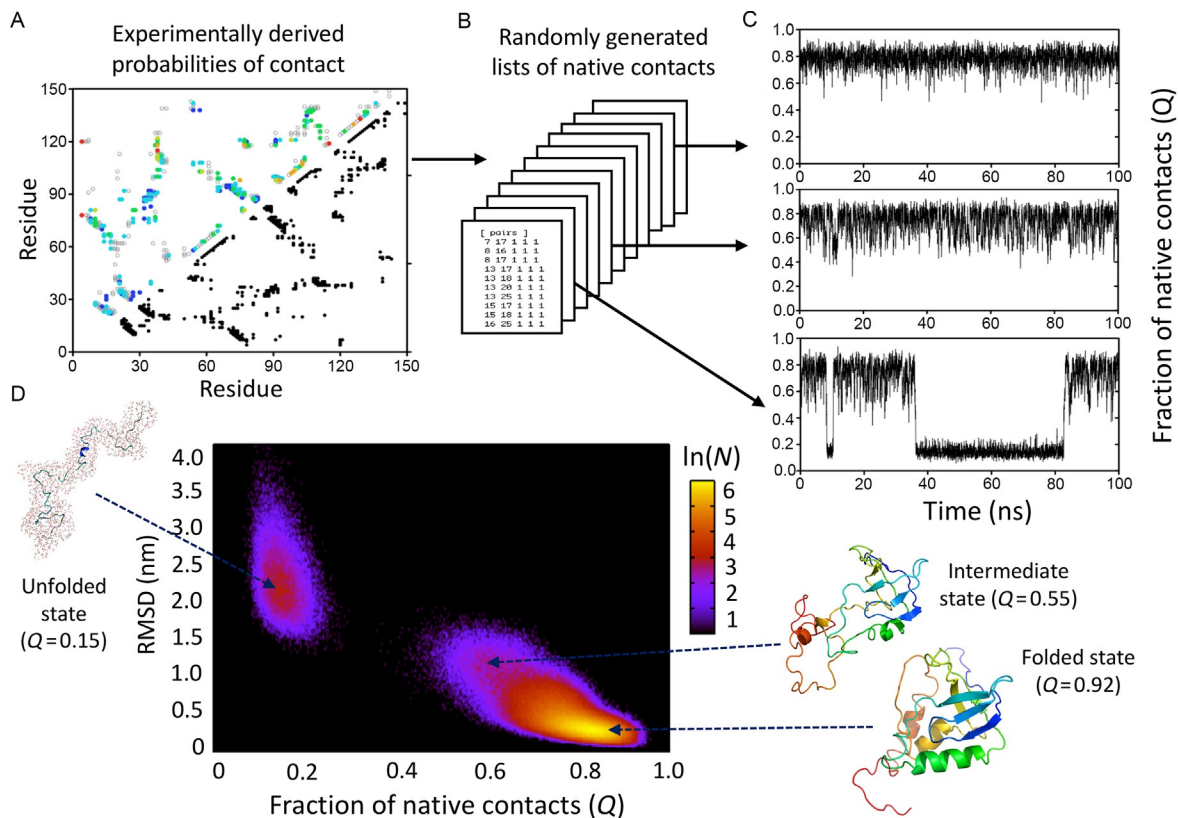
Fig. 7 Reconstruction of pseudo free-energy map from experimentally derived contact maps. (A and B) The contact map calculated at 800 bar from the residue-specific denaturation curves of Δ+PHS SNase in 1.8 M GuHCl is used to generate a list of native contacts. (C) These lists of native contacts are then used as input for a series of independent Go-model simulation. (D) The conformations generated by these simulations are collectively analyzed to reconstitute the free-energy landscape of the protein at a given pressure. In the example shown here, we observed the presence of a distinct intermediate state with a partially unfolded C-terminal subdomain (Roche, Caro, et al., 2012).

3.2 High-Pressure H/D Exchange

The early steps of unfolding can also be detected using H/D exchange measurements, a well-established NMR technique developed by Englander and coworkers (Roder, Elove, & Englander, 1988) and designed to identify distinct local stabilities in globular proteins. In such experiments, protonated samples are typically lyophilized and then quickly dissolved in D_2O buffer just prior to measurements. Series of HSQC spectra are then recorded and the decrease of individual cross–peak intensity is monitored over time, reflecting the exchange of amide protons with the deuterated buffer (Fig. 8). The hydrogen/deuterium exchange reaction is classically described as a two–step reaction characterizing a transient structural opening reaction of the protein that exposes an amine proton to the solvent (Englander & Kallenbach, 1983):

$$\text{Close}\,(H) \underset{k_{cl}}{\overset{k_{op}}{\longleftrightarrow}} \text{Open}\,(H) \overset{k_{rc}}{\longleftrightarrow} \text{Open}\,(D)$$
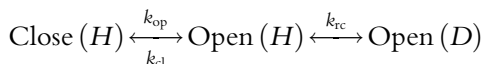
The steady-state exchange rate is given by:

$$k_{ex} = \frac{k_{op} k_{rc}}{k_{op} + k_{cl} + k_{rc}}$$

where the rate of exchange, k_{ex}, is calculated from the rate of the opening and closing reactions, k_{op} and k_{cl}, respectively, and the rate of exchange for a fully exposed amide proton, k_{rc}. Most commonly, exchange in proteins below pH 9 occurs through the so-called EX2-limit where $k_{cl} \gg k_{rc}$ and the H/D exchange rate is defined as:

$$k_{ex} = \frac{k_{op}}{k_{cl}} k_{rc} = k_{op} k_{rc}$$

In the EX2 condition, the H/D exchange rate provides the free energy for the underlying structural opening reaction:

$$\Delta G_x = -RT \ln K_{op} \text{ and } PF = \frac{1}{K_{op}} = \frac{k_{rc}}{k_{ex}}$$

The rate constant k_{ex} can be readily measured for each residue from the decrease in intensity of their corresponding cross-peak in the [^{1}H–^{15}N]-HSQC after dissolving the sample in D_2O buffer (Fig. 9). The effective equilibrium opening constant and corresponding protection factor (PF) is then obtained by normalizing k_{ex} by the intrinsic rate of exchange)
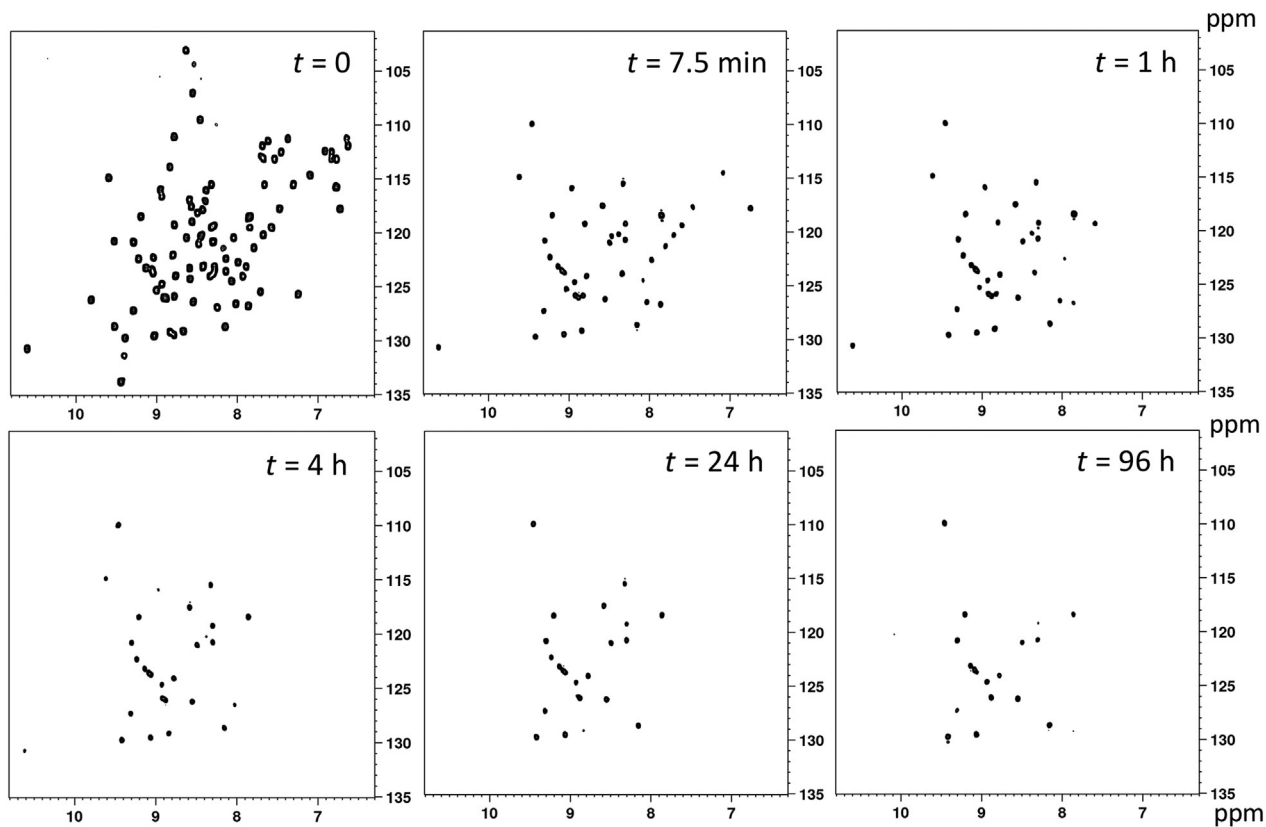
Fig. 8 Proton/deuteron amide exchange measurement on Titin I27 domain at atmospheric pressure. [^{1}H–^{15}N]-HSQC (7.5 min recording time) were recorded at 298 K over a period of 4 days after dissolving a freshly lyophilized sample of Titin I27 (same buffer conditions as stated in Fig. 1) in D_2O. The spectrum at time $t=0$ represents the reference spectrum recorded in H_2O before freeze-drying.
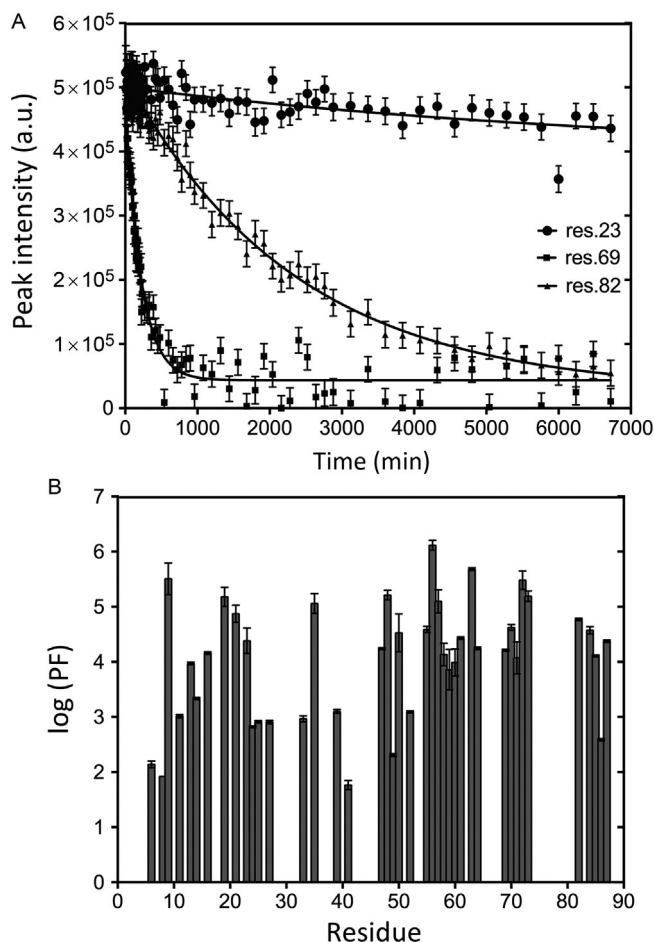
Fig. 9 Measurement of amide protecting factors (PF) from proton/deuteron exchange on Titin I27 domain at atmospheric pressure. (A) Measurement of the exchange rate constant k_{ex} on [^{1}H–^{15}N]-HSQC for three representative residues. (B) Plot of the protecting factors (PF) vs the protein sequence.

(Bai, Sosnick, Mayne, & Englander, 1995). The rates of exchange of fully solvent-exposed amide protons (k_{rc}) are determined for each amino acid on the basis of model peptide studies and depend on the neighboring residues types, the pH of the buffer and temperature at which the experiment is recorded (Bai, Milne, Mayne, & Englander, 1993). Fuentes and Wand combined for the first time the H/D exchange experiments with pressure perturbation to examine the energetics of the apocytochrome b562, introducing for this purpose an additional correction to account the effect of

pressure on the k_{rc} (Fuentes & Wand, 1998). With increasing pressure, they observed a systematic increase in the rate of exchange or equivalently, a decrease in the calculated protection factors. Apparent volume changes for exchange (ΔV_x) were estimated from the linear dependence of the free energy of exchange with pressure ($\Delta G_x(p) = \Delta G_x^0 + p\Delta V_x$). Using this method, they were able to identify three regions with distinct subglobal cooperative stabilities and pressure sensitivities (Fuentes & Wand, 1998). High-pressure H/D exchange experiments were also used in the case of the cavity variants of SNase showing considerable variations in the measured ΔV_x for the mutants, compared to the flat ΔV_x profile obtained for the pseudo wild type $\Delta + \text{PHS}$ (Roche, Dellarole, et al., 2012). In good agreement with equilibrium unfolding data, these H/D experiments revealed the major remodeling of the folding free-energy landscape in response to the introduction of cavity-creating mutations.

4. CHARACTERIZATION OF THE TSE IN THE FOLDING REACTION

As for steady-state measurement, pressure unfolding kinetics can benefit from multidimensional NMR, giving a residue-per-residue description of the TSE. In theory, such a description could be reached using the method proposed by Roche, Caro, et al. (2012) described earlier, based on the analysis of the probability of contacts between residues as determined from the denaturation curves measured at a residue level. Indeed, Fossat et al. (2016) successfully used this approach to fully map the entire folding landscape of the leucine-rich repeat protein, pp32 (Anp32), combining pressure-dependent site-specific ^1H–^{15}N HSQC data with coarse-grained molecular dynamics simulations. The results obtained using this equilibrium approach demonstrate that the main barrier to folding of pp32 is quite broad and lies near the unfolded state, with structure apparent only in the C-terminal region. Nevertheless, this approach, based on steady-state experiments, failed to provide information on the rate constants k_u and k_f associated to the folding process.

As with steady-state studies, a local description of the kinetic parameters and of the TSE should be, in principle, attainable through multidimensional NMR spectroscopy. Nevertheless, while multidimensional NMR experiments provide residue-specific structural information, their time resolution is limited (10–40 min for HSQC spectra). In cases for which folding is intrinsically sufficiently slow and folding activation volumes sufficiently

large (Royer, 2008; Vidugiris et al., 1995), pressure–jump can be combined with classical 2D NMR experiments, such as ^{1}H–^{15}N HSQC, to study folding kinetics, yielding local folding and unfolding rates for nearly every residue in a protein. This was done, for instance, on SNase and a series of variants with extremely slow relaxation times (up to 12 h) (Roche et al., 2013).

For proteins with faster relaxation times (<1 h), conventional ^{1}H–^{15}N HSQC can be replaced by 2D SOFAST-HMQC experiments (Schanda & Brutscher, 2005, Schanda, Forge, & Brutscher, 2007), that can be acquired in few tens of seconds. Such experiments were used to measure the local residue-specific relaxation times for several cavity-containing mutants of SNase. These experiments allow a residue-specific description of the TSE and of its molar volume, and thus internal cavity volume, relative to the folded and unfolded states (Fig. 10). In the case of the I92A SNase cavity-mutant, we also showed that the TSE molar volume was sensitive to the concentration of guanidinium chloride (Roche et al., 2013): increasing the concentration of this chaotropic reagent promoted the selection of higher volume conformers in the TSE, confirming the so-called Hammond effect (Matouschek & Fersht, 1993; Pappenberger, Saudan, Becker, Merbach, & Kiefhaber, 2000). In addition, the local description of the TSE revealed that cavity hydration concerns different regions of the protein, depending on the guanidinium concentration. The obvious limitation of the method presented above to obtain kinetics parameters of the folding reaction is the low time resolution of 2D NMR spectroscopy, even though this drawback has been at least partially circumvented by methodological developments (Frydman, Scherf, & Lupulescu, 2002; Gal, Schanda, Brutscher, & Frydman, 2007): HSQC-type experiments can be now recorded in less than a second, extending significantly the application of real-time spectroscopy.

The above approaches remain unsatisfactory to study subsecond folding kinetics, which is the case for most small globular proteins. In such cases, high-pressure relaxation dispersion experiments can be used to uncover the rate of exchange and thermodynamic properties of a two-state or three-state folding process on a millisecond timescale (Bezsonova, Korzhnev, Prosser, Forman-Kay, & Kay, 2006; Korzhnev et al., 2006; Tugarinov, Libich, Meyer, Roche, & Clore, 2015). Zhang et al. introduced the use of high-pressure ZZ-exchange experiments to investigate the transition states of protein folding, obtaining residue-specific folding rates for the two autonomous N-terminal and C-terminal domains of the ribosomal protein L9 (Zhang et al., 2016). These ZZ-exchange experiments also provide a
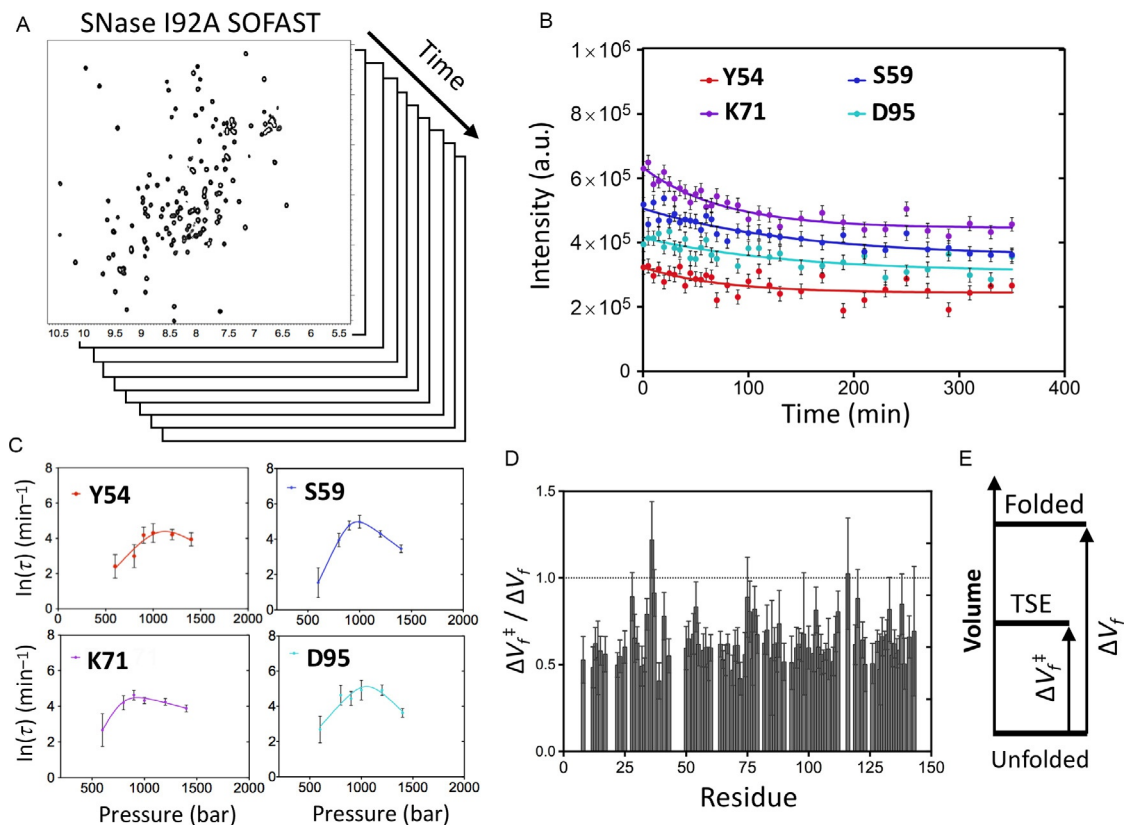
Fig. 10 Residue-specific hydration state of the transition state ensemble (TSE) of SNase I92A variant obtained through *p*-jump kinetic measurements. (A) Time series of SOFAST HMQC were recorded after 200 bar pressure jumps. (B) The intensity profiles of individual amide cross-peaks are then analyzed and fitted to obtain the value of $\tau_{(p)} = 1/(k_u + k_f)$ at a given pressure. (C) The plots of $\ln(\tau)$ vs pressure are finally fitted for each amide bond to extract the value of activation volume for folding ($\Delta V_f^{\ddagger}$). (D) The ratio of ΔV^0 at equilibrium to $\Delta V_f^{\ddagger}$ measured for SNase I92A are plotted as a function of the amino sequence, showing an average ratio of ca. 0.6 (E), indicating that the creation of a large cavity in the central core of the protein via the I92A substitution led to a major destabilization of the TSE (Roche et al., 2013).

relatively easy method to assign the ^{1}H/^{15}N chemical shifts of the pressure-induced denatured states (Zhang et al., 2016). Recently, Charlier et al. introduced a novel method for measuring the rate of exchange and chemical shifts of the folded, intermediate, and unfolded states induced by switching pressure on a millisecond timescale (Charlier et al., 2018). The new pressure-jump NMR apparatus is based on a spectrometer-controlled valve governing a reservoir of hydraulic fluid that can be rapidly and repeatedly opened/closed during the course of a 2D or 3D NMR experiment (Alderson, Charlier, Torchia, Anfinrud, & Bax, 2017; Charlier et al., 2018). This system is reminiscent of the pressure-jump apparatus originally designed by Kremer et al. for introducing pulsed pressure perturbation in 1D and 2D NMR experiments (Kremer et al., 2011).
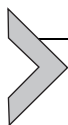
5. CONCLUSIONS

This chapter describes several NMR experiments that can be used in conjunction with high hydrostatic pressure to populate and characterize partially folded, excited states on protein folding landscapes. The experiments described range from simple one-dimensional proton spectra to more complex multidimensional kinetic schemes. NMR offers a myriad of further possibilities. We have not discussed characterization of pressure effects on protein dynamics by ^{2}H methyl relaxation and ^{15}N amide relaxation (Fu et al., 2012) or ^{13}C–^{1}H HSQC experiments to monitor local disruption of protein cores by the observation of folded state methyl group resonances. Residual dipolar couplings and NOEs can be measured at high pressure (Fu & Wand, 2013; Kitahara, Yokoyama, & Akasaka, 2005; Roche, Dellarole, et al., 2015; Roche, Louis, et al., 2015; Sibille, Dellarole, Royer, & Roumestand, 2014), providing complementary structural constraints on the intermediates populated. Nor have we described here the use of NMR-based DOSY diffusion measurements to characterize the intermolecular association of GMP at high pressure (Gao et al., 2017). Because pressure acts locally on biomolecules, leading to increased population of intermediates and excited states relative to other perturbation approaches, and because the NMR toolbox coupled with pressure offers such a wide range of approaches to probe multiple and complementary physical properties of biomolecules, we expect this approach to yield increasingly deeper insight into biomolecular sequence, structure–function relationships.

REFERENCES

Akasaka, K. (2006). Probing conformational fluctuations of proteins by pressure perturbation. *Chemical Reviews*, *106*, 1814–1835.

Akasaka, K., Kitahara, R., & Kamatari, Y. O. (2013). Exploring the folding energy landscape with pressure. *Archives of Biochemistry and Biophysics*, *531*, 110–115.

Alderson, T. R., Charlier, C., Torchia, D. A., Anfinrud, P., & Bax, A. (2017). Monitoring hydrogen exchange during protein folding by fast pressure jump NMR. *Journal of the American Chemical Society*, *139*, 11306–11309.

Ando, N., Barstow, B., Baase, W. A., Fields, A., Matthews, B. W., & Gruner, S. M. (2008). Structural and thermodynamic characterization of T4 lysozyme mutants and the contribution of internal cavities to pressure denaturation. *Biochemistry*, *47*, 11097–11109.

Bai, Y., Milne, J. S., Mayne, L., & Englander, S. W. (1993). Primary structure effects on peptide group hydrogen exchange. *Proteins*, *17*, 75–86.

Bai, Y., Sosnick, T. R., Mayne, L., & Englander, S. W. (1995). Protein folding intermediates—Native state hydrogen exchange. *Science*, *269*, 192–197.

Bezsonova, I., Korzhnev, D. M., Prosser, R. S., Forman-Kay, J. D., & Kay, L. E. (2006). Hydration and packing along the folding pathway of SH3 domains by pressure-dependent NMR. *Biochemistry*, *45*, 4711–4719.

Charlier, C., Alderson, T. R., Courtney, J. M., Ying, J., Anfinrud, P., & Bax, A. (2018). Study of protein folding under native conditions by rapidly switching the hydrostatic pressure inside an NMR cell. *Proceedings of the National Academy of Sciences of the United States of America*, *115*, E4169–E4178.

Dao, T. P., Majumdar, A., & Barrick, D. (2014). Capping motifs stabilize the leucine-rich repeat protein PP32 and rigidify adjacent repeats. *Protein Science*, *23*, 801–811.

de Oliveira, G. A., & Silva, J. L. (2015). A hypothesis to reconcile the physical and chemical unfolding of proteins. *Proceedings of the National Academy of Sciences of the United States of America*, *112*, E2775–E2784.

Dellarole, M., & Royer, C. A. (2014). High-pressure fluorescence applications. *Methods in Molecular Biology*, *1076*, 53–74.

Englander, S. W., & Kallenbach, N. R. (1983). Hydrogen exchange and structural dynamics of proteins and nucleic acids. *Quarterly Reviews of Biophysics*, *4*, 521–655.

Englander, S. W., Mayne, L., & Krishna, M. M. G. (2007). Protein folding and misfolding: Mechanism and principles. *Quarterly Reviews of Biophysics*, *40*, 287–326.

Fossat, M. J., Dao, T. P., Jenkins, K., Dellarole, M., Yang, Y. S., McCallum, S. A., et al. (2016). High-resolution mapping of a repeat protein folding free energy landscape. *Biophysical Journal*, *111*, 2368–2376.

Frach, R., Kibies, P., Bottcher, S., Pongratz, T., Strohfeldt, S., Kurmann, S., et al. (2016). The chemical shift baseline for high pressure NMR spectra of proteins. *Angewandte Chemie International Edition*, *55*, 8757–8760.

Frydman, L., Scherf, T., & Lupulescu, A. (2002). The acquisition of multidimensional NMR spectra within a single scan. *Proceedings of the National Academy of Sciences of the United States of America*, *99*, 15858–15862.

Fu, Y., Kasinath, V., Moorman, V. R., Nucci, N. V., Hilser, V. J., & Wand, A. J. (2012). Coupled motion in proteins revealed by pressure perturbation. *Journal of the American Chemical Society*, *134*, 8543–8550.

Fu, Y., & Wand, A. J. (2013). Partial alignment and measurement of residual dipolar couplings of proteins under high hydrostatic pressure. *Journal of Biomolecular NMR*, *56*, 353–357.

Fuentes, E. J., & Wand, A. W. (1998). Local stability and dynamics of apocytochrome b562 examined by the dependence of hydrogen exchange on hydrostatic pressure. *Biochemistry*, *37*, 9877–9883.

Gal, M., Schanda, P., Brutscher, B., & Frydman, L. (2007). UtraSOFAST HMQC NMR and repetitive acquisition of 2D protein spectra at Hz rates. *Journal of the American Chemical Society*, *129*, 1372–1377.

Gao, M., Harish, B., Berghaus, M., Seymen, R., Arns, L., McCallum, S. A., et al. (2017). Temperature and pressure limits of guanosine monophosphate self-assemblies. *Scientific Reports*, *7*, 9864.

Ishima, R., Torchia, D. A., & Louis, J. M. (2007). Mutational and structural studies aimed at characterizing the monomer of HIV-1 protease and its precursor. *The Journal of Biological Chemistry*, *282*, 17190–17199.

Kamatari, Y. O., Kitahara, R., Yamada, H., Yokoyama, S., & Akasaka, K. (2004). High-pressure NMR spectroscopy for characterizing folding intermediates and denatured states of proteins. *Methods*, *34*, 133–143.

Kitahara, R., Yokoyama, S., & Akasaka, K. (2005). NMR snapshots of a fluctuating protein structure: Ubiquitin at 30 bar–3 kbar. *Journal of Molecular Biology*, *347*, 277–285.

Korzhnev, D. M., Bezsonova, I., Evanics, F., Taulier, N., Zhou, Z., Bai, Y., et al. (2006). Probing the transition state ensemble of a protein folding reaction by pressure-dependent NMR relaxation dispersion. *Journal of the American Chemical Society*, *128*, 5262–5269.

Kremer, W., Arnold, M., Munte, C. E., Hartl, R., Erlach, M. B., Koehler, J., et al. (2011). Pulsed pressure perturbations, an extra dimension in NMR spectroscopy of proteins. *Journal of the American Chemical Society*, *133*, 13646–13651.

Lindberg, M. O., & Oliveberg, M. (2007). Malleability of protein folding pathways: A simple reason for complex behaviour. *Current Opinion in Structural Biology*, *17*, 21–29.

Louis, J. M., & Roche, J. (2016). Evolution under drug pressure remodels the folding free-energy landscape of mature HIV-1 protease. *Journal of Molecular Biology*, *428*, 2780–2792.

Matouschek, A., & Fersht, A. R. (1993). Application of physical organic chemistry to engineered mutants of proteins: Hammond postulate behavior in the transition state of protein folding. *Proceedings of the National Academy of Sciences of the United States of America*, *90*, 7814–7818.

Myers, J. K., Pace, C. N., & Scholtz, J. M. (1995). Denaturant m values and heat capacity changes: Relation to changes in accessible surface areas of protein unfolding. *Protein Science*, *4*, 2138–2148.

Naganathan, N., & Munoz, V. (2008). Determining denaturation midpoints in multiprobe equilibrium protein folding experiments. *Biochemistry*, *47*, 6752–6761.

Pappenberger, G., Saudan, C., Becker, M., Merbach, A. E., & Kiefhaber, T. (2000). Denaturant-induced movement of the transition state of protein folding revealed by high-pressure stopped-flow measurements. *Proceedings of the National Academy of Sciences of the United States of America*, *97*, 17–22.

Peterson, R. W., & Wand, J. A. (2005). Self-contained high-pressure cell, apparatus, and procedure for the preparation of encapsulated proteins dissolved in low viscosity fluids for nuclear magnetic resonance spectroscopy. *The Review of Scientific Instruments*, *76*, 094101.

Privalov, P. L., & Gill, S. J. (1988). Stability of protein structure and hydrophobic interaction. *Advances in Protein Chemistry*, *39*, 191–234.

Ravindra, R., & Winter, R. (2003). On the temperature-pressure free-energy landscape of proteins. *Chemphyschem*, *4*, 359–365.

Roche, J., Caro, J. A., Norberto, D. R., Barthe, P., Roumestand, C., Schlessman, J. L., et al. (2012). Cavities determine the pressure unfolding of proteins. *Proceedings of the National Academy of Sciences of the United States of America*, *109*, 6945–6950.

Roche, J., Dellarole, M., Caro, J. A., Guca, E., Norberto, D. R., Yang, Y. S., et al. (2012). Remodeling of the folding free-energy landscape of staphylococcal nuclease by cavity-creating mutations. *Biochemistry*, *51*, 9535–9546.

Roche, J., Dellarole, M., Caro, J. A., Norberto, D. R., Garcia, A. E., Garcia-Moreno, B., et al. (2013). Effect of internal cavities on folding rates and routes revealed by real-time pressure-jump NMR spectroscopy. *Journal of the American Chemical Society*, *135*, 14610–14618.

Roche, J., Dellarole, M., Royer, C. A., & Roumestand, C. (2015). Exploring the protein folding pathway with high-pressure NMR: Steady-state and kinetics studies. *Sub-Cellular Biochemistry*, *72*, 261–278.

Roche, J., Louis, J. M., Bax, A., & Best, R. B. (2015). Pressure-induced structural transition of mature HIV-1 protease from a combined NMR/MD simulation approach. *Proteins: Structure, Function, and Bioinformatics*, *83*, 2117–2123.

Roder, H., Elove, G. A., & Englander, S. W. (1988). Structural characterization of folding intermediates in cytochrome-c by H-exchange labeling and proton NMR. *Nature*, *335*, 700–704.

Rouget, J. B., Aksel, T., Roche, J., Saldana, J. L., Garcia, A. E., Barrick, D., et al. (2011). Size and sequence and the volume change of protein folding. *Journal of the American Chemical Society*, *133*, 6020–6027.

Royer, C. A. (2008). The nature of the transition state ensemble and the mechanisms of protein folding: A review. *Archives of Biochemistry and Biophysics*, *469*, 34–45.

Sadqi, M., Fushman, D., & Muñoz, V. (2006). Atom-by-atom analysis of global downhill protein folding. *Nature*, *442*, 317–321.

Schanda, P., & Brutscher, B. (2005). Very fast two-dimensional NMR spectroscopy for real-time investigation of dynamic events in proteins on the time scale of seconds. *Journal of the American Chemical Society*, *127*, 8014–8015.

Schanda, P., Forge, V., & Brutscher, B. (2007). Protein folding and unfolding studied at atomic resolution by fast two-dimensional NMR spectroscopy. *Proceedings of the National Academy of Sciences of the United States of America*, *104*, 11257–11262.

Sibille, N., Dellarole, M., Royer, C., & Roumestand, C. (2014). Measuring residual dipolar couplings at high hydrostatic pressure: Robustness of alignment media to high pressure. *Journal of Biomolecular NMR*, *58*, 9–16.

Tugarinov, V., Libich, D. S., Meyer, V., Roche, J., & Clore, G. M. (2015). The energetics of a three-state protein folding system probed by high-pressure relaxation dispersion NMR spectroscopy. *Angewandte Chemie, International Edition*, *54*, 11157–11161.

Vidugiris, G. J. A., Markley, J. L., & Royer, C. A. (1995). Evidence for a molten globule-like transition state in protein folding from determination of activation volumes. *Biochemistry*, *34*, 4909–4912.

Zhang, Y., Berghaus, M., Klein, S., Jenkins, K., Zhang, S., McCallum, S. A., et al. (2018). High-pressure NMR and SAXS reveals how capping modulates folding cooperativity of the pp32 leucine-rich repeat protein. *Journal of Molecular Biology*, *430*, 1336–1349.

Zhang, Z., Kitazawa, S., Peran, I., Stenzoski, N., McCallum, S. A., Raleigh, D. P., et al. (2016). High pressure ZZ-exchange NMR reveals key features of protein folding transition states. *Journal of the American Chemical Society*, *138*, 15260–15266.